Experimental Damage Diagnosis of a Model Three-Story Spatial Frame

S. Sabatino[1], E. K. Ervin[2]

[1] Lehigh University, The Center for Advanced Technology for Large Structural Systems (ATLSS), 117 ATLSS Drive Bethlehem, PA 18015
[2] University of Mississippi, 106 Carrier Hall, P.O. Box 1848 University, MS 38677

ABSTRACT

Structural damage can be induced by a variety of events from short-term abnormal stresses to long-term natural aging. Detection of changes in a structure's ability to withstand subsequent loads can aid decisions on safety, repair, rehabilitation, and demolition. Dynamic property shifts can show internal cracks and minor damage before propagation or failure occurs, but only if a proper indicator is selected. In order to evaluate potential damage indices, a three-story metal frame building was constructed. Using Star Modal software, dynamic structural properties were obtained from modal decomposition on experimental tap test responses. The natural frequencies and mode shapes of the structure established an as-built baseline for comparison to ten other scenarios with removed bracing. Once modal properties for each case were determined, six unique damage indicators were applied to identical experimental data via twelve algorithms. The effectiveness of each damage detection technique was assessed, and final recommendations for the three-story model building were made. Of all the implemented algorithms, frequency response function (FRF) subtraction using the FRFs as a direct indicator is the most accurate damage detection scheme for the three-story test structure.

1 MOTIVATION

Engineers need to assess the "health" state of structures and ultimately improve the overall safety and reliability of infrastructure. Damage can occur in a structure as various forms, including member cracks, loosened joints, metal fatigue, and temporal deterioration. Additionally, damage can be caused by an assortment of loadings, including but not limited to aging and abnormal, sudden stresses such as an earthquake or terrorist attack. One can compare an undamaged "healthy" structure to one that has been significantly altered via load (the "damaged" structure) in order to observe changes in material properties. Material properties (i.e. stiffness and density) as well as dynamic parameters (i.e. natural frequencies and mode shapes) directly affect how the structure moves and may significantly alter response data collected from a particular structure.

In order to detect damage within a structure, engineers instrument it with sensors in order to collect data that can be utilized to calculate its global dynamic parameters. Field data may be obtained from more conventional sensors, such as accelerometers, strain gauges, and displacement transducers, or even newer instrumentation involving piezoelectrics or optical measures. With any experimental data set, the preliminary step in structural health evaluation includes analyzing an undamaged as-built structure in order to establish the baseline structural dynamic properties. Once information is gathered and processed about the baseline case, subsequent damage can theoretically be detected based solely on the collected data. If the structure is periodically monitored and data is collected on a regular basis, damage from both abnormal stresses and long-term aging effects can be detected. Once damage is identified and quantified within a structure, officials can decide to repair, rehabilitate, or demolish.

In order to evaluate the effectiveness of potential damage indicators, a three-story spatial frame structure made of steel and aluminum was constructed. Dynamic structural parameters were obtained from the measured response of the test building. An accelerometer was placed at the top of one of the columns comprising the structure in order to capture the building's response to a roving hammer's impulse signals. Twenty-six hammer hits were

performed and the responses were measured in two dimensions, resulting in a total of fifty-two measured FRF signals. Next, modal decomposition was utilized to obtain the natural frequencies and mode shapes of the structure. Once all required data were acquired for the structure, baseline structural dynamic properties of the test building were calculated.

After a baseline, "healthy," or undamaged state of the structure was established, damage was incrementally applied to the building by removing various members. A total of ten damage scenarios with significant structural modifications were examined. Once all properties for each damage case were determined, various damage indicators were applied. Finally, after the application of several damage detection methods, the effectiveness of each technique was evaluated and compared. Final recommendations for the three-story spatial frame were then made based on the results of all damage indicators.

2 EXPERIMENTAL SETUP

A three-story spatial frame, single bay structure was constructed from steel and aluminum in order to test and determine the relative effectiveness of several damage detection algorithms (**Fig. 1**). The columns are comprised of four continuous 0.3175 cm (1/8-inch) aluminum angles with 2.54 cm (1 inch) flanges, measuring 60.96 cm (24 inches) in height. The foundation of the structure consists of two stainless steel 12.70 cm (5") flanges bolted to each column and fastened to a massive granite table. Three 0.0508 cm (0.02") thick steel shim sheet squares measuring approximately 10.16 cm by 10.16 cm (4" by 4") are fastened to the columns 15.24 cm, 35.56 cm, and 55.88 cm (6", 14", and 22") from the base. The shim sheets represent three floors and are bolted in each corner to a column with two small 1.27 cm (0.5") flanges. Cross bracing is externally added within each story along all four faces. All sixteen cross bracing members are made using 0.0381 cm (0.015") thick, 1.27 cm (0.5") wide steel strips, each measuring approximately 30.5 cm (12 inches) in length.

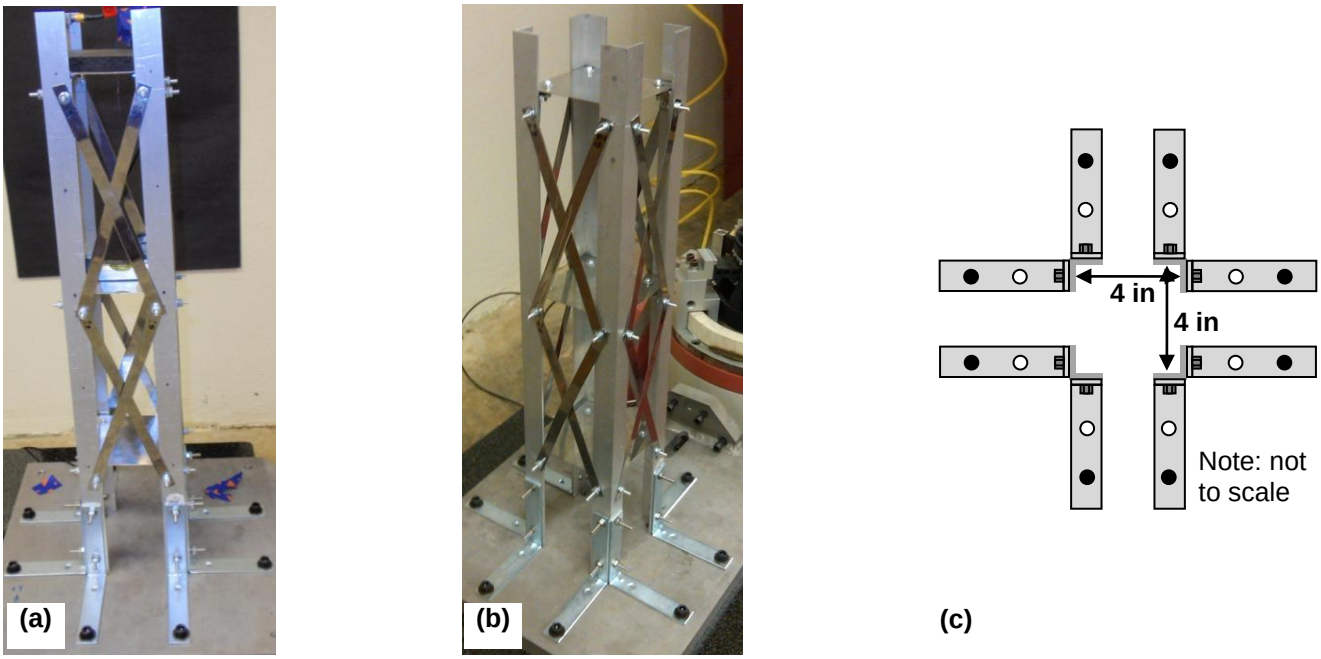

Fig. 1 Three-story spatial frame structure (a) side view, (b) isometric view and (c) plan view

A schematic of the experimental set up for impact hammer tap tests is shown in **Fig. 2**. A PCB-086C03 modally tuned impact hammer with 2.25 mV/N sensitivity is connected via a BNC cable to the National Instruments (NI) cDAQ-9172 data acquisition system. A Dytran 3055B1 tri-axial accelerometer with the following sensitivities: 100.7 mV/g (X), 99.1 mV/g (Y), and 101.9 mV/g (Z), is also connected to the DAQ system with BNC cables. The DAQ is connected via USB to a desktop PC that runs NI Labview which captures the signals created by the impact hammer and the response of the tap at the accelerometer. The triaxial accelerometer was placed at point 28 on the structure and acceleration was measured in both the X and Y directions, as indicated in **Fig. 2**. The

impact hammer was used to excite the building at twenty-six different locations, including the corners of all floors as well as the driving point 28. More specifically, taps were performed on the following points in both the X and Y directions: 5, 6, 7, 8, 13, 14, 15, 16, 21, 22, 23, 24, and 28. Impacts that included double hits or ones that did not produce a well-formed sine pulse were discarded. Acceleration data was recorded for a duration of 1 second and was sampled at 50,000 samples per second for each impact.

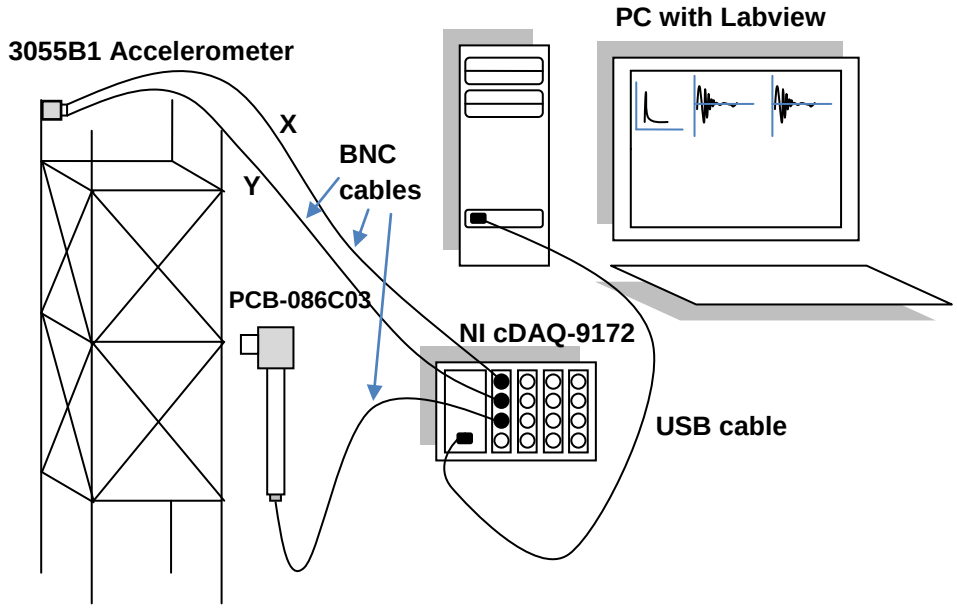

Fig. 2 Experimental setup

A wireframe model of the test structure with numeric labels assigned to each node is depicted in **Fig. 3**. Several damage scenarios were implemented in order to simulate real-world stiffness losses, environmental occurrences, and structural aging. All sixteen cross bracing members were progressively removed, creating configurations that incorporated symmetric, asymmetric, single story, and multiple story damage. The aforementioned data collection and data processing methods were carried out on all remaining damage cases.

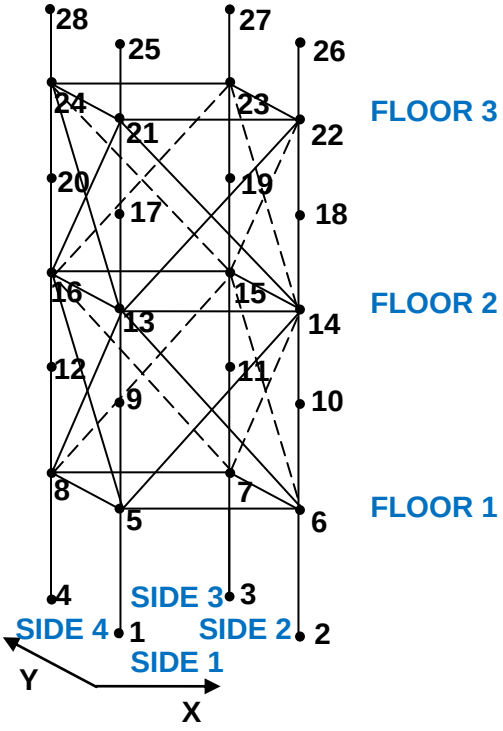

Fig. 3 Wireframe model (not to scale)

Table 1 summarizes all damage scenarios by providing lists of removed members and configuration descriptions. Cross braces are labeled by the two nodes from **Fig. 3** that each member spans. Bold typeface represents a member that was removed between two consecutive damage cases. For example, member 8-15 is bold for DC 1 and not for DC 2; this is because member 8-15 was removed for DC 1 and remained off in DC 2.

Table 1 Damage summary of scenarios

Damage Case (DC)	Members Removed (node-to-node)	Short Description
DC 0	None	Undamaged (baseline)
DC 1	8-15	Single story asymmetric damage with one brace removed
DC 2	8-15, **6-13**	Single story symmetric damage with one brace removed
DC 3	8-15, **7-16**	Single story asymmetric damage with two braces removed
DC 4	8-15, 7-16, **5-14**, **6-13**	Single story symmetric damage with two braces removed
DC 5	8-15, 5-14, 6-13, 7-16, **6-15**, **7-14**, **8-13, 5-16**	Single story symmetric damage with all first level cross bracing removed
DC 6	8-15, 5-14, 6-13, 7-16, 6-15, 7-14, 8-13, 5-16, **15-24**	Multiple story asymmetric damage with one brace removed
DC 7	8-15, 5-14, 6-13, 7-16, 6-15, 7-14, 8-13, 5-16, 15-24, **14-21**	Multiple story symmetric damage with one brace removed
DC 8	8-15, 5-14, 6-13, 7-16, 6-15, 7-14, 8-13, 5-16, 15-24, 14-21, **13-22, 16-23**	Multiple story symmetric damage with two braces removed
DC 9	8-15, 5-14, 6-13, 7-16, 6-15, 7-14, 8-13, 5-16, 15-24, 14-21, 13-22, 16-23, **14-23, 15-22**	Multiple story asymmetric damage with two braces removed
DC 10	8-15, 5-14, 6-13, 7-16, 6-15, 7-14, 8-13, 5-16, 15-24, 14-21, 13-22, 16-23, 14-23, 15-22, **13-24, 16-21**	Multiple story symmetric damage with all cross bracing removed

3 RESULTS

After all impact data sets were collected for each damage case, the files were fed through several data processing software programs that correctly manipulated the data into a form accepted by Star Modal. Star Modal is a modal analysis/decomposition software package that matches collected data to a 3-D model, taking structural geometry into account. However, it requires specific formatting and requires processing via Mathematica and Matlab in order to ensure proper layout and to calculate the frequency response functions, respectively. The first five global modes of vibration are selected by the user and are based on several parameters, including the relative size of its modal peak, its shape animation, as well as frequency and damping stability. The natural frequencies of the first five modes for all eleven cases are summarized in **Table 2**.

Table 2 Experimentally identified natural frequencies in Hertz for all damage cases

Mode	DC 0	DC 1	DC 2	DC 3	DC 4	DC 5	DC 6	DC 7	DC 8	DC 9	DC 10
1	73.55	51.83	49.27	61.22	42.15	38.98	37.16	23.04	24.28	26.56	18.77
2	91.77	85.28	87.09	86.23	--	52.76	53.12	52.42	51.51	31.4	27.3
3	177.59	162.46	148.99	161.4	126.92	127.43	127.2	70.44	73.26	71.62	53.64
4	211.89	209.82	210.3	213.16	213.64	216.66	195.19	179.16	204.26	204.57	197.09
5	236.54	237.57	233.99	230.1	229.71	234.07	231.23	233.07	228.03	219.66	211.48

For damage case 0, the first experimental global mode occurs at 73.55 Hz. This mode shape is the first bending mode in the X direction; the structure is generally swaying along the X direction. The columns spanning points 3-17 and 4-18 show the most motion along the X direction. The second mode shape is a Y direction sway and occurs at 91.77 Hz. At 177.59 Hz, the third experimental mode occurs and is identified as the first torsion mode due to the twisting of the structure depicted by model animation. The fourth mode occurs at 211.89 Hz and the model animation shows the second bending mode in the X direction. The last fifth mode appears at 236.54 Hz and its animation depicts the second bending mode in the Y direction.

A modal peaks map is constructed and displayed in **Fig. 4**. The dependent axis in these waterfall plots represents the magnitude-normalized cumulative FRF of each damage case. **Fig. 4** illustrates a decrease in natural frequencies as the structure becomes more damaged. With progression from DC 0 to DC 10, damage increases and the structure becomes more flexible due to the removal of cross-bracing members. This phenomenon is observed when comparing all eleven damage cases and validates the results of modal decomposition for incremental damage. However, one exception to this rule occurs when comparing DC 2 to DC 3. Since one cross bracing member was removed while one was reattached, it is reasonable to witness an increase in the stiffness of the structure for the sequential scenario of DC 2 vs. DC 3. Due to the increase in stiffness, mode 1's natural frequency also shifts upward. In addition to shifts in natural frequencies, modal peak splitting also occurs within **Fig. 4**. The dashed arrows point to peaks that represent a weaker form of the mode indicated by the solid arrow of the same color. For example, mode 3 in DC 1 has two possible locations, one at approximately 160 Hz that was identified as the stronger form of torsion, and one at 150 Hz whose mode shape is not as distinctive as the mode at 160 Hz. It is likely that these are not separate modes, just the one torsion mode at 175 Hz in DC 0 splitting into two modes in DC 1. Peak splitting is a direct result of damage and can help identify structural weakness within a system.

4 DAMAGE DETECTION METHODS

Twelve different algorithms involving six major damage indices have been applied to the same experimental data. The analyzed damage indicators include MAC (modal assurance criterion), COMAC (coordinate modal assurance criterion), modal curvature methods, flexibility-based algorithms, story stiffness approximations, and direct FRF comparisons. Each of these damage indicators were applied for both sequential and cumulative damage. Sequential damage scenarios include incremental modifications that result in small damage steps. Conversely, cumulative damage scenarios are ones that incorporate a large amount of stiffness loss, i.e. DC 0 vs. DC 9.

Any suspect experimental data was eliminated before implementing damage detection methods. Since the second mode for DC 4 was unable to be identified, DC 4 is eliminated as a suitable damage case. A complete set of damage indices cannot be formed since DC 4 is missing critical mode shape data for the first bending mode in the Y direction. Additionally, DC 10 is removed from the damage diagnosis due to poor data fidelity. Despite well-defined mode shapes, initial damage indicator testing shows that DC 10 produces undesirable results with a relatively high amount of noise and false positives. This could be due to the significant structural flexibility and weak column coupling. With DC 4 and DC 10 removed from the damage indicator analysis, a total of seven sequential and one cumulative damage scenarios are examined.

Several observations on damage prediction results from sequential case comparison. Multiple methods are most sensitive towards the top of the structure; COMAC, flexibility division, story stiffness, FRF subtraction, and FRF division identified most damage as occurring above the second floor. In addition, there are several algorithms that indicate a significant amount of damage within the torsion mode. These methods include curvature division, flexibility division, story stiffness, FRF subtraction, and FRF division. Finally, the COMAC of curvatures index is not adequate for use on sequential damage scenarios because it does not accurately locate damage.

The cumulatively damaged case shows similarities between detection methods. Minimal damage is predicted by COMAC of curvatures, curvature division, and flexibility division. These methods do not accurately depict true damage and are deemed inadequate for the test structure. Conversely, several algorithms tend to accurately identify damage. COMAC, story stiffness, FRF subtraction, and FRF division methods are among those that indicate a significant amount of damage throughout the test structure. Note that false positives cannot be correctly identified as damage should be indicated throughout the entire model building.

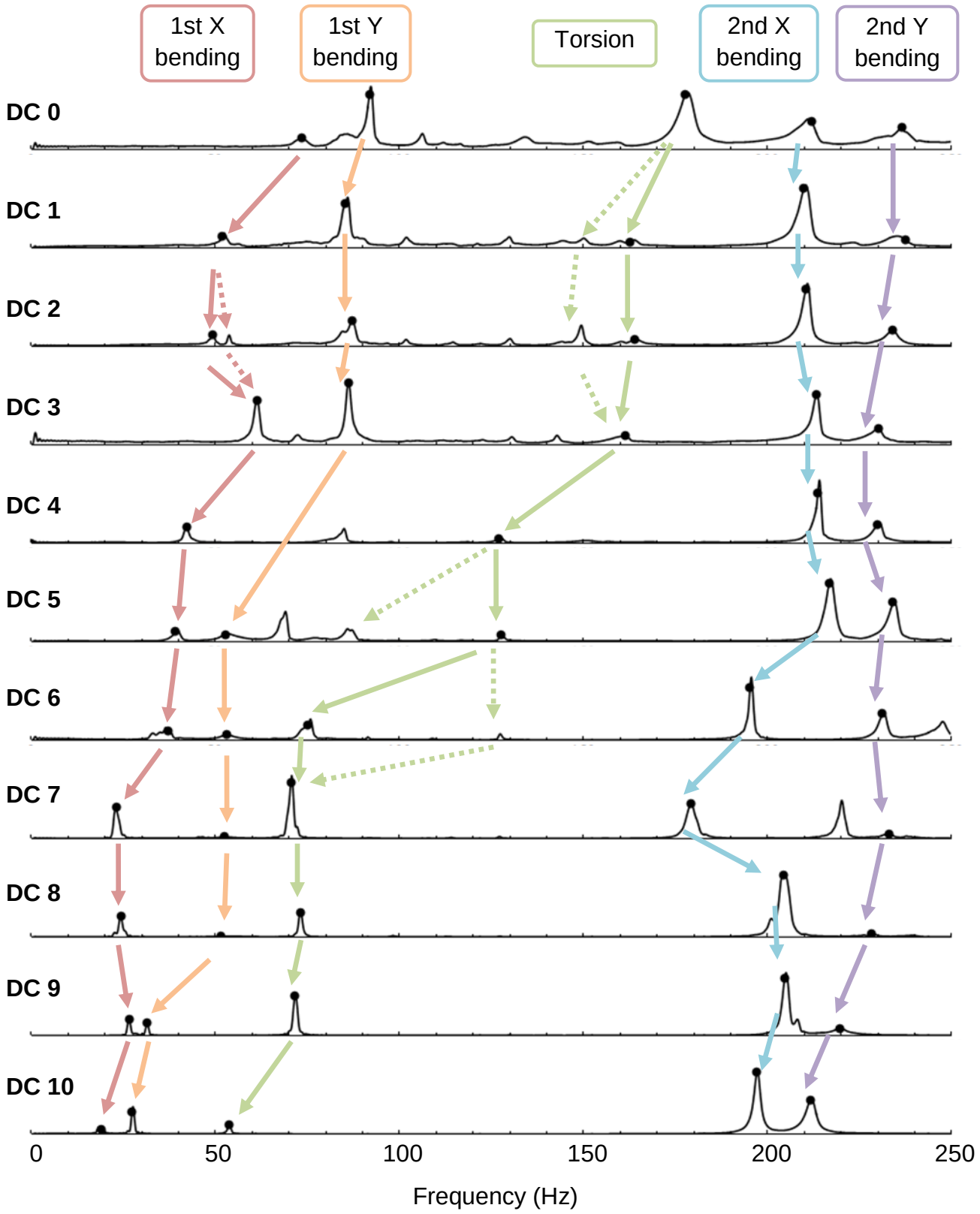

Fig. 4 Mode map for all damage cases; five modes identified and potential split pairs are shown by dashed arrows

5 CONCLUSIONS

In order to evaluate potential damage indices, a three-story metal frame building was constructed. Dynamic structural properties were obtained from modal decomposition on experimental tap test responses. The natural frequencies and mode shapes of the structure established an as-built baseline for comparison to ten other scenarios with removed bracing. Once modal properties for each case were determined, six unique damage indicators were applied to identical experimental data via twelve algorithms. The effectiveness of each damage detection technique was assessed. Of all the implemented algorithms, FRF subtraction using the FRFs as a direct indicator is the most accurate damage detection scheme for the three-story test structure.

ACKNOWLEDGEMENTS

This work was supported by the National Science Foundation [BRIGE 08242277] and the Mississippi Space Grant Consortium Graduate Research Fellowship.